Dalton Transactions

ROYAL SOCIETY OF CHEMISTRY

COMMUNICATION

View Article Online
View Journal | View Issue

Check for updates

Cite this: *Dalton Trans.*, 2024, **53**, 903

Received 26th November 2023,
Accepted 21st December 2023

DOI: 10.1039/d3dt03954d

rsc.li/dalton

Open Access Article. Published on 22 December 2023. Downloaded on 2/20/2026 2:34:25 AM.
This article is licensed under a Creative Commons Attribution 3.0 Unported Licence.

Nitroiminotriazole (NIT) based potential solid propellants: synthesis, characterization, and applications†

Sohan Lal, [a] Richard J. Staples [b] and Jean'ne M. Shreeve *[a]

Nitroimino (R = N-NO_2) energetic material is a unique class of high energy density materials (HEDM). Synthesis and characterization of insensitive nitroimino compounds are a major challenge. Here triazole-based nitroimino compounds and their high-nitrogen green energetic salts in excellent yields are described. These materials exhibit high positive heats of formation (7.84 to 735.29 kJ mol^{-1}), good densities (1.66 to 1.98 g cm^{-3}), suitable detonation properties (P = 22.02 to 31.88 GPa; D = 7472 to 8936 ms^{-1}) and high ballistic properties (I_{sp} 205.66 to 295.35 s; C^* = 1065 to 1832 ms^{-1}) with good thermal (T_d = 136–378 °C) and mechanical stabilities (IS = 10–40 J and FS = 120–360 N).

Developing new energetic materials with balanced performance which involves design, synthesis, characterization, and testing is a major challenge for the scientific community.[1–4] *Ab initio*-based calculations demonstrate energetic performance of the materials, which helps in the design of novel materials with emergent properties.[5] Choosing a suitable ring system (backbone) with appropriate explosophoric group substituents results in potential energetic materials. Ideal energetic materials exhibit high density, high energetic performance and excellent thermal stability while concomitantly generating gaseous products of low toxicity during the combustion process.[6] High nitrogen five-membered heterocycles are an attractive choice in designing potential high energy density materials (HEDM) because of their high positive heats of formation. The design, synthesis, and applications of nitroimino-containing materials as important explosophoric groups are receiving more and more attention.[7] Some interesting examples such as (3*E*,5*E*)-3,5-dinitramide-ylidene-1,2,4-triazolidine (**1**, **DNAT**),[8] (*E*)-*N*-(3-amino-1,2,4-oxadiazol-5(4*H*)-ylidene)-nitramide (**2**, **AODANA**),[9] *N*-(1,4-dihydro-5*H*-tetrazol-5-ylidene)-nitramide (**3**, **DHTzNA**),[10] and (*E*)-*N*-(1-(nitroamino)-1,4-dihydro-5*H*-tetrazol-5-ylidene)-nitramide (**4**, **DHTNANA**)[11] are known (Fig. 1). Now, the synthesis and characterization of versatile high nitrogen energetic salts of triazole, namely (*E*)-*N*-(2,4-dihydro-3*H*-1,2,4-triazol-3-ylidene)-nitramide (**5**, **DHTNA**) and (4-(nitroamino)-4*H*-1λ^4,2,4-triazole-3,5-diyl) bis(ethane-2,1-diyl) dinitrate (**6**, **BEDNINAT**), are described.

Commercially available 4*H*-1,2,4-triazol-3-amine **7** was treated with mixed acid (100% HNO_3 and 98% H_2SO_4) to give 2,4-dihydro-3*H*-1,2,4-triazol-3-ylidene-nitramine (**5**, **DHTNA**)[12] in excellent yield (Scheme 1).

Subsequently, **5** was treated with different bases ($NH_2NH_2{\cdot}H_2O$, $NH_2OH{\cdot}H_2O$, aqueous NH_3, KOH, NaOH) in aqueous solution to form the corresponding energetic salts in quantitative yield. When 3-hydroxypropanenitrile **13** was treated with hydrazine monohydrate in the presence of sulfur powder, 2,2′-(4-amino-4*H*-1,2,4-triazole-3,5-diyl)-bis(ethan-1-ol) (**14**, **ATBE-ol**) resulted in good yield. Compound **14** was further nitrated to form (4-(nitroamino)-4*H*-1λ^4,2,4-triazole-3,5-diyl)-bis(ethane-2,1-diyl) dinitrate (**6**, **BEDNINAT**).

All new compounds are solids at room temperature. Their thermal stabilities were determined using differential scanning calorimetry (DSC) and thermogravimetric analysis (TGA) at the heating rate of 5 °C min^{-1}, respectively (ESI, Fig. S49–S64†). Notably, all new compounds exhibit good thermal stabi-

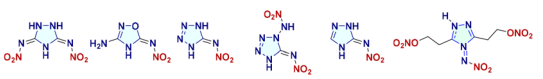

	DNAT, 1	AODANA, 2	DHTzNA, 3	DHTNANA, 4	DHTNA, 5 This work	BEDNINAT, 6 This work
Nitrogen (%)	51.85	48.27	64.61	58.95	54.26	31.92
Oxygen (%)	33.84	33.08	24.60	33.67	24.79	41.67
$\Delta H_f°$ (kJmol^{-1})	194.00	-196.30	264.00	486.30	150.25	735.29
P (GPa)	34.30	25.60	36.30	43.40	26.85	31.88
D (km/s)	8880	8033	9173	9967	8311	8553
ρ (g/cm^3)	1.83	1.70	1.87	1.93	1.78	1.67
T_m/T_d (°C)	--/125	114/168	--/122	--/110	--/205	128/136
IS (J)	≥4	≥40	≥1.5	≥1	≥30	≥15
FS (N)	---	≥360	≥8	≥5	≥240	≥120

Fig. 1 Triazole, tetrazole and oxadiazole-containing nitroimino energetic materials.[8–11]

[a]*Department of Chemistry, University of Idaho, Moscow, Idaho, 83844-2343, USA. E-mail: jshreeve@uidaho.edu; Fax: (+1) 208-885-5173*
[b]*Department of Chemistry, Michigan State University, East Lansing, Michigan 48824, USA*

†Electronic supplementary information (ESI) available. CCDC 2296314–2296316 and 2303917. For ESI and crystallographic data in CIF or other electronic format see DOI: https://doi.org/10.1039/d3dt03954d

Open Access Article. Published on 22 December 2023. Downloaded on 2/20/2026 2:34:25 AM.
This article is licensed under a Creative Commons Attribution 3.0 Unported Licence.

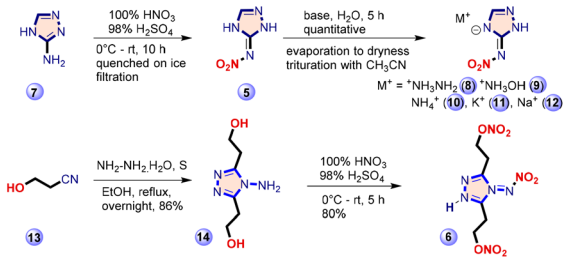

Scheme 1 Synthesis of the title compounds.

lities (T_d = 205–378 °C), except compound **6** (T_d = 136 °C), enhancing their possible utility for solid rocket propulsion.

Compound **5**·H_2O recrystallized by the slow evaporation of an aqueous solution in the monoclinic space group $P2_1$ with a density of 1.740 g cm^{-3} at 100 K with a half molecule in the asymmetric unit, which is characterized by the sum formula, Z is 1, and Z' is 0.5 (Fig. 2 and ESI, Tables S4–S9†). Compound **6** was recrystallized by the slow evaporation of methanol. It crystallizes in the orthorhombic space group *Pbca* with a density of 1.699 g cm^{-3} at 100 K with one molecule in the asymmetric unit, which is characterized by the sum formula, Z is 8, and Z' is 1. The relatively high density is supported by various types of interactions such as intermolecular H-bonds and π–π-interactions. The H-bonding interplay has a maximum D–D distance of 3.1 Å and a minimum angle of 110° are present in **6**: N1–O1_1: 2.685 Å.

Compound **11** was crystallized by the slow evaporation of water in the monoclinic space group *P*21/*c* and has an excellent density of 2.009 g cm^{-3} (at 100 K) and 1.983 g cm^{-3} (at 25 °C), which are supported by the intermolecular H-bonds and metal organic framework (MOF) formed in the molecule. The H-bonding interplay has a maximum D–D distance of 3.1 Å and a minimum angle of 110° are present in **11**: N1–O2: 2.624 Å, N1–N3_1: 2.924 Å. (Fig. 2 and ESI, Tables S15–S19†). Compound **14** was recrystallized by the slow evaporation of methanol. It crystallizes in the monoclinic space group *P*21/*n* with a density of 1.428 g cm^{-3} at 100 K with one molecule in the asymmetric unit, which is characterized by the sum formula, Z is 4, and Z' is 1. (Fig. 2 and ESI, Tables S20–S24†).

The measurement of available oxygen after all hydrogen atoms are converted to H_2O and all carbon atoms into CO or CO_2 [oxygen balance (OB, Ω)], plays an important role in the combustion process. The new compounds have negative oxygen balances (OB^{CO_2} = −54.75% to −9.57%), which are superior to TNT (OB^{CO_2} = −73.97%). These materials have a high density (1.66 g cm^{-3} to 1.98 g cm^{-3}) superior to TNT (ρ = 1.65 g cm^{-3}) and RDX (ρ = 1.80 g cm^{-3}). The potassium salt (**11**) has the highest density (1.98 g cm^{-3}) which is comparable to CL-20 (ρ = 2.04 g cm^{-3}) (Table 1).

The heats of formation ($\Delta H_f°(s)$) of the new compounds were calculated with the Gaussian 03 suite of programs[13] using the isodesmic method (Fig. S1†). Corresponding ballistic and detonation properties were calculated using ($\Delta H_f°(s)$) and experimental densities with the help of EXPLO5 V7.01 software.[14] Compounds **6**, **8** and **9** exhibit high positive enthalpies of formation ($\Delta H_f°(s)$), 735.29 kJ mol^{-1}, 297.69 kJ mol^{-1} and 198.07 kJ mol^{-1}, respectively, whereas compound **11** has the lowest ($\Delta H_f°(s)$, 7.84 kJ mol^{-1}) (Table 1).

A comprehensive comparison of the ballistic properties of the new materials shows that compounds **6**, **8** and **9** have excellent potential as solid rocket propellants. Composite propellants (with AP/Al/HTPB) performed better than those of individual neat mono-propellant compounds. Compounds **11** and **12**·H_2O exhibit promising explosive properties, as given in Table 1. Additionally, the ballistic properties (I_{sp} and C^*) of compound **6** were estimated at different compositions of ADN and AP (Fig. S67†).

The physicochemical properties of materials are directly allied with their molecular structures. Hirshfeld surfaces and 2D-fingerprints were calculated and visualized with CrystalExplorer 21.5 software,[15] which show that compounds **6** and **11** are rigidly packed and their high densities are governed by numerous types of interactions as shown in Fig. 3. In Hirshfeld surface analysis, red and blue dots on the compound surfaces illustrate high and low close contacts, respectively Fig. 3a. Fingerprint plots suggest that O–H contacts for compounds **6** (~57.4%), **11** (~18.5%) and N–H contacts for compounds **6** (~6.3%), **11** (~16.9%), are contributing to the high stability of compound **11**. On the other hand, the high number of various close interactions such as N–N, O–O and O–N contacts in the molecules, result in high-impact sensitivity.[16] Their measured impact sensitivities also support this result, and the stability order is RDX < **6** < **11** (Table 1). The electrostatic potentials (ESP) of compounds **6** and **11** were predicted with Multiwfn and VMD software,[17] The positive fraction (red) and a negative fraction (blue) represent the less and more active sites on the molecule surface, respectively (Fig. 4).

The potassium cation of compound **11** and the hydrocarbon chain in compound **6** are present under red surfaces, showing that they provide additional stability to the material.

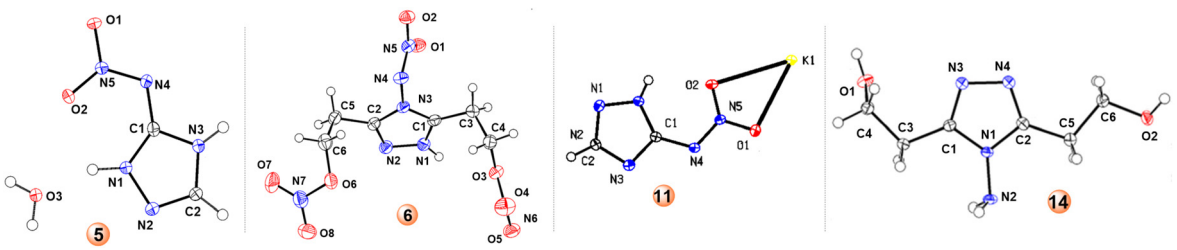

Fig. 2 Single crystal X-ray structure (thermal ellipsoid plot (50%)) of **5**·H_2O, **6**, **11** and **14**.

This journal is © The Royal Society of Chemistry 2024

Open Access Article. Published on 22 December 2023. Downloaded on 2/20/2026 2:34:25 AM.
This article is licensed under a Creative Commons Attribution 3.0 Unported Licence.

Table 1 Comparison of physicochemical properties of **5–12** with AP, TNT and TKX-50

Compound	**5**	**6**	**8**	**9**	**10**	**11**	**12**·H_2O	AP[a]	TNT[b]	TKX-50[b]
T_m/T_d[c] [°C]	—/205	128/136	—/211	—/213	—/218	—/260	—/378	—/200	—/300	—/221
ρ[d] [g cm^{-3}]	1.78	1.67	1.69	1.69	1.66	1.98	1.96	1.95	1.65	1.88
ΔH_f[e] [kJ mol^{-1} kJ^{-1} g^{-1}]	150.25/ 1.16	735.29/ 2.39	297.69/ 1.85	198.07/ 1.22	142.38/ 0.97	7.84/ 0.05	80.83/ 0.54	−295.80/- 2.51	−59.30/−0.26	213.40/ 0.90
OB^{CO}[f] (%)	−18.85	−13.02	−34.76	−19.74	−32.85	−28.71	−31.77	34.04	−24.66	−13.60
OB^{CO2}[g] (%)	−43.38	−44.27	−54.62	−39.48	−54.75	−9.57	−10.59	34.04	−73.97	−27.10
N[h] [%]	54.26	31.92	60.85	51.84	57.72	41.89	46.36	54.47	18.50	59.31
N + O[i] [%]	79.05	73.59	80.71	81.45	79.62	61.03	67.54	66.39	60.76	86.41
P[j] [GPa]	26.85	31.88	29.52	29.05	25.26	22.02	27.34	18.43	18.56	36.74
D[k] [ms^{-1}]	8311	8553	8936	8674	8359	7472	8359	6858	6817	9592
$-Q$[l] [kJ kg^{-1}]	4263	7256	4838	5256	4154	4076	4775	1433	4363	4744
IS[m] [J]	30	10	40	40	40	10	10	15	15	20
FS[n] [N]	240	120	360	360	360	120	120	360	353	120
I_{sp}[o,t] [s]	218.46	294.49	234.49	250.46	216.34	176.77	194.85	156.63	206.49	243.64
rI_{sp}[p,t] [s]	388.86	491.80	396.29	423.28	359.12	357.07	381.91	306.15	341.54	457.32
C^*[q,t] [ms^{-1}]	1372.20	1832.5	1467.7	1578.1	1334.0	1065.3	1165.4	976.8	1283.5	1531.2
I_{sp}[r,t] [s]	239.65	295.35	255.63	270.23	244.63	205.66	213.24	232.00	235.53	267.83
I_{sp}[s,t] [s]	228.62	248.37	243.31	249.19	234.99	197.48	192.85	262.11	225.11	244.44

[a] Ref. 1 and 14. [b] Ref. 6 and 14. [c] Melting point and decomposition temperature (onset) under nitrogen gas (DSC, 5 °C min^{-1}). [d] Measured densities, gas pycnometer at room temperature. [e] Calculated heat of formation. [f] Oxygen balance based on CO. [g] Oxygen balance based on CO_2. [h] Nitrogen content in %. [i] N + O contents in %. [j] Calculated detonation velocity. [k] Calculated detonation pressure. [l] Heat of detonation. [m] Measured impact sensitivity. [n] Measured friction sensitivity. [o] Specific impulse of neat compound (monopropellant). [p] Density specific impulse of neat compound (monopropellant). [q] Characteristic velocity. [r] Specific impulse at 88% compound and 12% Al. [s] Specific impulse at 78% compound, 12% Al (fuel additive) and 10% binder (HTPB). [t] Specific impulse calculated at an isobaric pressure of 70 bar and initial temperature of 3300 K using EXPLO5 V 7.01.

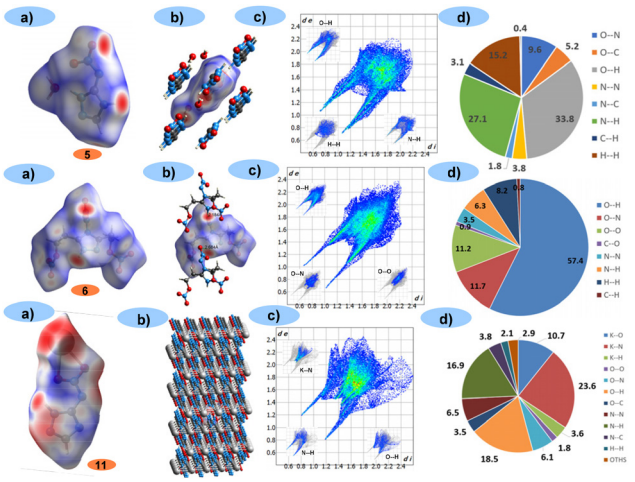

Fig. 3 (a) Hirshfeld surfaces in crystal stacking for **5**, **6**, and **11** (b) Arrangement in crystal packing. (c and d) 2D- fingerprint and individual contribution of close contacts.

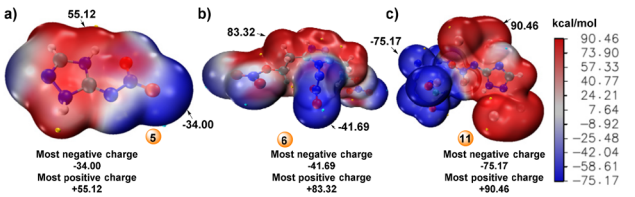

Fig. 4 Molecular surface (ESP map) of compounds **5** (a), **6** (b) and **11** (c).

ESP minima and maxima for compounds **5**, **6**, and **11** are −34.00, −41.69, −75.17 kcal mol^{-1} and +55.12, +83.32, 90.46 kcal mol^{-1}, respectively.

Numerous non-covalent interactions and reduced density gradients were determined in compounds **5**, **6**, and **11** using B3LYP/6-311++G(d,p) level of theory as illustrated in Fig. 5. It is clear that compound **11** has high numbers of interactions and fewer steric effects compared to **5** and **6**, resulting in high thermal stability.

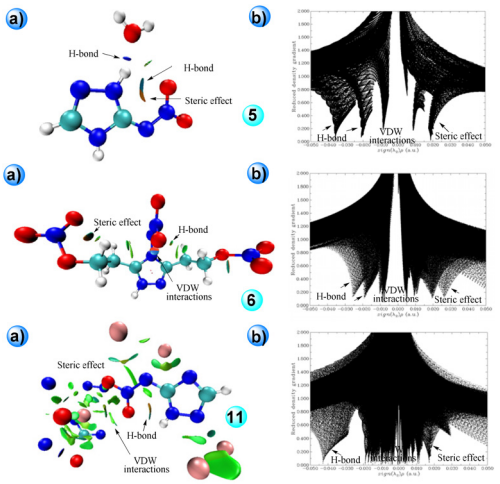

Fig. 5 (a) Non-covalent interactions (NCI). (b) Reduced density gradients (RDG) and scatter diagrams of **5**, **6** and **11**.

Open Access Article. Published on 22 December 2023. Downloaded on 2/20/2026 2:34:25 AM.
This article is licensed under a Creative Commons Attribution 3.0 Unported Licence.

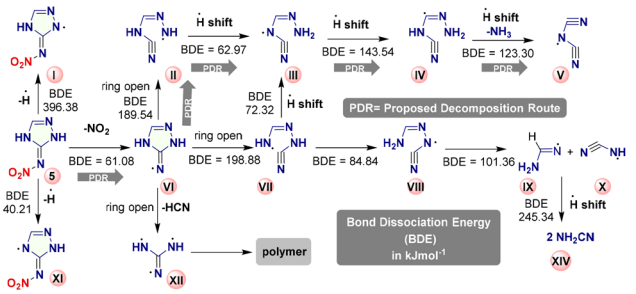

Fig. 6 Proposed thermal decomposition route for **5**.

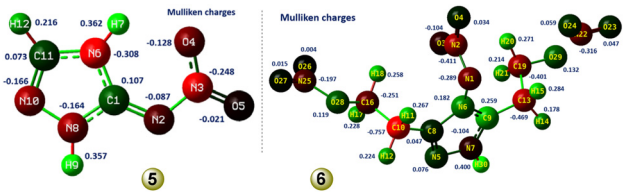

Fig. 7 Mulliken charges on compounds **5** and **6**.

Additionally, to better understand the decomposition of **5** during the combustion process, the bond dissociation energy (BDE, gas-phase) of homolytic cleavage of various bonds was calculated at B3LYP/6-311++G(d,p) level of theory (Fig. 6).

Based on BDEs, compound **5** would decompose according to PDR (see Fig. 6), path will follow **5** to intermediate **VI–II–III–IV** and **V**. The charge distribution on the molecule is determined in terms of Mulliken's charges, as shown in Fig. 7. C1 and N2 in compound **5** and C9 and N6 in compound **6** are the most positively charged carbon and nitrogen atoms in the molecules. Overall, charges are delocalized on the whole molecule, supporting their high stability.

The detonation properties of the new compounds were calculated using EXPLO5 V 7.01 program[14b] and their solid-phase heats of formation and experimental densities, and results are given in Table 1. Compounds **5** (P = 26.85 GPa, D = 8311 ms^{-1}, Q = 4263 kJ kg^{-1}), **6** (P = 31.88 GPa, D = 8553 ms^{-1}, Q = 7256 kJ kg^{-1}), **8** (P = 29.52 GPa, D = 8936 ms^{-1}, Q = 4838 kJ kg^{-1}) and **9** (P = 29.05 GPa, D = 8674 ms^{-1}, Q = 5256 kJ kg^{-1}), which are comparable to those of RDX (D = 8801 ms^{-1}, P = 33.60 GPa, Q = 5728 kJ kg^{-1}), TNT (D = 6817 ms^{-1}, P = 18.56 GPa, Q = 4363 kJ kg^{-1}) and AP (D = 6858 ms^{-1}, P = 18.43 GPa, Q = 1413 kJ kg^{-1}).

Compounds **6**, **10**, and **11** have low sensitivities[18] (IS = 10 J, FS = 120 N), which make them potential secondary explosives. Whereas compounds **6** (I_{sp} = 295.35 s, C^* = 1832 ms^{-1}), and **9** (I_{sp} = 270.23 s, C^* = 1578 ms^{-1}) show superior specific impulse (I_{sp}) and characteristic velocity (C^*) than the TNT (I_{sp} = 235.53 s, C^* = 1283 ms^{-1}) and TKX-50 (I_{sp} = 267.83 s, C^* = 1531 ms^{-1}), making them potential solid fuels for rocket propulsion. Additionally, more insights to design a laser ignition setup for the new compounds, their UV-visible spectra of compounds **5** and **6** were predicted at B3LYP/6-311++G(d,p) level, (see, ESI, Fig. S65 and S66†).

In summary, a facile synthesis of **DHTNA** and its energetic salts from commercially available 3-nitro-1*H*-1,2,4-triazole was developed. The new compounds were fully characterized by FTIR, NMR, and elemental analyses. The structures of **5**·H_2O, **6**, **11**, and **14** were also confirmed by single-crystal X-ray analysis. A comprehensive study of the energetic properties and thermal behaviour of the new compounds was also carried out. Compounds **5–12** possess excellent thermal stabilities (T_d, 136–378 °C) and low sensitivities to impact (10–40 J) and friction (120–360 N). Compound **6** melts (T_m, 128 °C) before decomposition (T_d, 136 °C) and exhibits detonation properties (P = 31.88 GPa, D = 8553 ms^{-1}), which makes it a promising candidate as a green explosive. Compounds **6** (P = 31.88 GPa, D = 8553 ms^{-1}, I_{sp} = 295.35 s, C^* = 1832.5 ms^{-1}), **8** (P = 29.52 GPa, D = 8936 ms^{-1}, I_{sp} = 255.63s, C^* = 1467.7 ms^{-1}) and **9** (P = 29.05 GPa, D = 8674 ms^{-1}, I_{sp} = 270.23s, C^* = 1578.1 ms^{-1}) have excellent potential as solid propellants in rocket propulsion.

Author contributions

S. L. investigation, methodology, conceptualization, and manuscript writing. R. J. S. X-ray data collection and structure solving. S. L. and J. M. S. conceptualization, manuscript writing-review and editing, supervision.

Conflicts of interest

The authors declare no competing financial interest.

Acknowledgements

The Rigaku Synergy S Diffractometer was purchased with support from the National Science Foundation MRI program (1919565). We are grateful for the support of the Fluorine-19 fund.

References

1 (*a*) J. P. Agrawal, *High Energy Materials: Propellants, Explosives and Pyrotechnics*, Wiley-VCH, Weinheim, 1st edn, 2010; (*b*) S. Lal, R. J. Staples and J. M. Shreeve, FOX-7 derived nitramines: Novel propellants and oxidizers for solid rocket propulsion, *Chem. Eng. J.*, 2023, **468**, 143737; (*c*) S. Lal, R. J. Staples and J. M. Shreeve, FOX-7 based nitrogen-rich green energetic salts: Synthesis, characterization, propulsive and detonation performance, *Chem. Eng. J.*, 2023, **452**, 139600.

2 (*a*) S. Lal, R. J. Staples and J. M. Shreeve, Design and synthesis of high-performance planar explosives and solid propellants with tetrazole moieties, *Org. Lett.*, 2023, **25**, 5100–5104.

 This journal is © The Royal Society of Chemistry 2024

Open Access Article. Published on 22 December 2023. Downloaded on 2/20/2026 2:34:25 AM. This article is licensed under a Creative Commons Attribution 3.0 Unported Licence.

3 (*a*) S. R. Yocca, M. Zeller, E. F. C. Byrd and D. G. Piercey, 1, 5-Diaminotetrazole-4N-oxide (SYX-9): a new high-performing energetic material with a calculated detonation velocity over 10 kms^{-1}, *J. Mater. Chem. A*, 2022, **10**, 1876–1884; (*b*) A. Sankaranarayanan, S. Lal, S. Rashmi, I. N. N. Namboothiri, A. Chowdhury and N. Kumbhakarna, Droplet combustion studies on novel cage hydrocarbons using colar-ratio pyrometry, *Fuel*, 2020, **282**, 118816.

4 (*a*) J. R. Yount, M. Zeller, E. F. C. Byrd and D. G. Piercey, 4,4′,5,5′-Tetraamino-3,3′-azo-bis-1,2,4-triazole and the electrosynthesis of high-performing insensitive energetic materials, *J. Mater. Chem. A*, 2020, **8**, 19337–19347.

5 (*a*) S. Lal, H. Gao and J. M. Shreeve, Design and computational insight into two novel CL-20 analogues, BNMTNIW and BNIMTNIW: High performance energetic materials, *New J. Chem.*, 2022, **46**, 16693–16701; (*b*) J. Zhou, J. Zhang, B. Wang, L. Qiu, R. Xu and A. B. Sheremetev, Recent synthetic efforts towards high energy density materials: How to design high performance energetic structures, *Fire Phys. Chem.*, 2022, **2**, 83–139.

6 H. Gao and J. M. Shreeve, Azole-based energetic salts, *Chem. Rev.*, 2011, **111**, 7377–7436.

7 Y. Wang, L. Hu, S. Pang and J. M. Shreeve, Nitroimino as an energetic group in designing energetic materials for practical use, a tautomerism from nitroamino, *J. Mater. Chem. A*, 2023, **11**, 13876–13888.

8 A. M. Astakhov, D. V. Antishin, V. A. Revenko, A. D. Vasiliev and E. S. A. Buka, Simple method for the preparation of 3,5-dinitrimino-1,2,4-triazole and its salts, *Chem. Heterocycl. Compd.*, 2017, **53**, 722–727.

9 Y. Tang, H. Gao, L. A. Mitchell, D. A. Parrish and J. M. Shreeve, Enhancing energetic properties and sensitivity by incorporating amino and nitramino groups into a 1,2,4-oxadiazole building block, *Angew. Chem., Int. Ed.*, 2016, **55**, 1147–1150.

10 J. Stierstorfer and T. M. Klapötke, Nitration products of 5-amino-1H-tetrazole and methyl-5-amino-1H-tetrazoles-Structures and properties of promising energetic materials, *Helv. Chim. Acta*, 2007, **90**, 2132–2150.

11 D. Fischer, T. M. Klapötke and J. Stierstorfer, 1,5-Di(nitramino)tetrazole: High sensitivity and superior explosive performance, *Angew. Chem., Int. Ed.*, 2015, **54**, 10299–10302.

12 For preliminary data: T. P. Kofman, G. Y. Kartseva and M. B. Shcherbinin, Synthesis, structure, and alkylation of 4-nitroamino-1,2,4-triazole, *Russ. J. Org. Chem.*, 2002, **38**, 1343–1350.

13 M. J. Frisch, G. W. Trucks, H. B. Schlegel, G. E. Scuseria, *et al.*, *Revision D.01 ed*, Gaussian Inc., Wallingford CT, 2003.

14 (*a*) N. Fischer, D. Fische, T. M. Klapötke, D. G. Piercey and J. Stierstorfer, Pushing the limits of energetic materials-the synthesis and characterization of dihydroxylammonium 5, 5′-bistetrazole-1, 1′-diolate, *J. Mater. Chem.*, 2012, **22**, 20418–20422; (*b*) M. Suceska, *EXPLO5, version 6.01*, Brodarski Institute, Zagreb, Croatia, 2013.

15 P. R. Spackman, M. J. Turner, J. J. McKinnon, S. K. Wolff, D. J. Grimwood, D. Jayatilaka and M. A. Spackman, CrystalExplorer: A program for Hirshfeld surface analysis, visualization and quantitative analysis of molecular crystals, *J. Appl. Crystallogr.*, 2021, **54**, 1006–1011.

16 (*a*) S. Lal, R. J. Staples and J. M. Shreeve, Design and synthesis of phenylene-bridged isoxazole and tetrazole-1-ol based energetic materials of low sensitivity, *Dalton Trans.*, 2023, **52**, 3449–3457; (*b*) H. Gao, Q. Zhang and J. M. Shreeve, Fused heterocycle-based energetic materials (2012–2019), *J. Mater. Chem. A*, 2020, **8**, 4193–4216.

17 T. Lu and F. Chen, Multiwfn: A multifunctional wavefunction analyzer, *J. Comput. Chem.*, 2012, **33**, 580–592.

18 NATO, standardization agreement 4487 (STANAG4487), explosives, friction sensitivity tests 2002.